ACS SyntheticBiology

Research Article

pubs.acs.org/synthbio

Orthogonal Labeling of M13 Minor Capsid Proteins with DNA to Self-Assemble End-to-End Multiphage Structures

Gaelen T. Hess,[†,‡,¶] Carla P. Guimaraes,[§,¶] Eric Spooner,[§] Hidde L. Ploegh,*[,§,∥] and Angela M. Belcher*[,†,‡,⊥]

[†]The David H. Koch Institute for Integrative Cancer Research, [‡]Department of Materials Science and Engineering, [∥]Department of Biology, and [⊥]Department of Biological Engineering, Massachusetts Institute of Technology, Cambridge, Massachusetts 02139, United States

[§]Whitehead Institute for Biomedical Research, Cambridge, Massachusetts 02142, United States

Supporting Information

ABSTRACT: M13 bacteriophage has been used as a scaffold to organize materials for various applications. Building more complex multiphage devices requires precise control of interactions between the M13 capsid proteins. Toward this end, we engineered a loop structure onto the pIII capsid protein of M13 bacteriophage to enable sortase-mediated labeling reactions for C-terminal display. Combining this with N-terminal sortase-mediated labeling, we thus created a phage scaffold that can be labeled orthogonally on three capsid proteins: the body and both ends. We show that covalent attachment of different DNA oligonucleotides at the ends of the new phage structure enables formation of multiphage particles oriented in a specific order. These have potential as nanoscale scaffolds for multi-material devices.

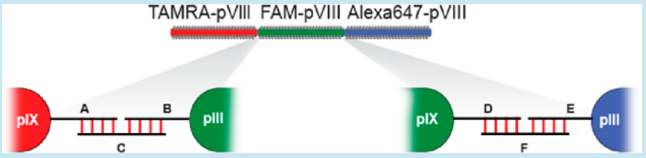

KEYWORDS: *DNA, orthogonal labeling, protein engineering, self-assembly, sortase*

A major goal of synthetic biology is to control and program biological molecules to perform a desired function, such as the organization of materials to create devices.[1] In this context, the self-assembling capsid proteins of M13 bacteriophage have been explored to form nanowire structures,[2,3] which have been used to build battery and solar devices.[4,5] M13 bacteriophage is an attractive building block for more complex multimaterial devices such as transistors and diodes, because its major capsid protein (pVIII) can been engineered to bind and nucleate different materials.[2,4,6]

The building of more complex materials requires construction of multiphage scaffolds, but this has been hampered by the inability to freely manipulate the major capsid protein located in the body of phage and the four minor capsid proteins located at the ends of the phage (pIII, pVI, pVII, pIX) to form specific connections between different M13 particles. Streptavidin-based conjugates[6−8] and leucine zippers[9] have been explored to connect virions through the pIII, pVIII, or pIX proteins, but the resultant structures neither displayed a 1:1 stoichiometry, as streptavidin can bind up to four biotin molecules, nor did they allow precise control over structure length.[9]

DNA hybridization is a commonly used strategy to establish nanoscale connections. It has been used to order spherical viruses[10,11] and order gold nanoparticles into crystal lattices.[12,13] Although these and polymer-based particles can be conjugated with DNA,[14,15] the use of M13 offers two main advantages: high aspect ratio scaffolds and five proteins that may be engineered for different functions. Cross-linking individual M13 phage particles by means of DNA hybridization would have several advantages: first, a 1:1 stoichiometry with easier control over the number of phage coming together at a single connection; second, specificity and versatility, as the sequence of a DNA oligonucleotide can be modified to form new orthogonal complementary pairs; and third, reversible ligations, as DNA−DNA interactions can be disrupted by heat and reformed by cooling.

We accomplished specific labeling of the N-termini of pIII and pIX, with a variety of substituents using the sortase enzyme from *Staphylococcus aureus* ($SrtA_{aureus}$).[7] Sortase-catalyzed transpeptidation reactions comprise two steps. Initial recognition of an LPXTG motif placed near the C-terminus of a polypeptide that $SrtA_{aureus}$ cleaves after the threonine residue to form a thioester-linked acyl-enzyme intermediate. This is followed by a nucleophilic attack by the α-amine of an oligoglycine (poly)peptide, which resolves the intermediate. Because the LPXTG motif-containing (poly)peptide can be conjugated beforehand with any substituent of choice (e.g., fluorophore), the final product is the protein of interest, in this case pIII or pIX, labeled at the N-terminus with that substituent. The $SrtA_{aureus}$-catalyzed reactions are orthogonal to *Streptococcus pyogenes* sortase A ($SrtA_{pyogenes}$)-mediated labeling of pVIII, as the enzyme recognizes an LPXTA motif and the intermediate is resolved by an N-terminal double alanine nucleophile[7,16] instead of the $(Gly)_n$ preferred by $SrtA_{aureus}$.

Received: February 27, 2013
Published: May 28, 2013

Here we describe the installation of a loop structure comprising the LPXTG sortase recognition motif on pIII to enable C-terminal display. Using an M13 construct containing three sortase labeling motifs within the same virion, we demonstrate orthogonal labeling of pIII, pVIII, and pIX proteins. Using this construct, we built end-to-end multiphage structures in a specific order by labeling the pIII and pIX proteins with DNA and different fluorophores on the pVIII.

RESULTS AND DISCUSSION

C-Terminal Phage Vector Display of the Sortase Substrate Motif. We first examined whether we could display the LPXTG sortase-recognition motif at the C-terminus of the pIII, pVI, or pIX proteins. Although genetic engineering of the M13 phage genome (Supporting Note 1) yielded the desired modifications as confirmed by PCR (Supplementary Figure 1), they were incompatible with phage assembly.

We then engineered the N-terminus of pIII to display a 50-amino-acid sequence composed of an LPETG recognition motif for $SrtA_{aureus}$ flanked by two cysteines. When these cysteines engage in disulfide bond formation, they form a loop similar to that displayed by the subunit A of cholera toxin.[17] Because proteolytic cleavage of the loop improves labeling efficiency,[17] we inserted a linker followed by a Factor Xa protease cleavage site immediately downstream of the LPETG motif (Figure 1a). We confirmed that sortase, pIII, pIX, and pVIII remained intact upon incubation with Factor Xa (data not shown). Thus, only the engineered pIII is a substrate for Factor Xa. This phage construct will be referred to hereafter as loopXa-pIII.

C-Terminal Sortase-Mediated Labeling of pIII. We labeled the loopXa-pIII phage construct at pIII with a GGGK(TAMRA) peptide using $SrtA_{aureus}$ (Figure 1b). Factor Xa was included in the reaction. We analyzed the samples by SDS-PAGE under both reducing and nonreducing conditions, followed by fluorescent imaging and immunoblotting with an anti-pIII antibody. Only under nonreducing conditions and when all four reaction components were present did we observe a 60 kDa fluorescent anti-pIII reactive protein (Figure 1b), consistent with the presence of an intramolecular disulfide bond and loop formation on a single pIII molecule.

Sortase-mediated transpeptidation reactions afford attachment of a wide range of molecules to this loop structure, including a preassembled protein complex of ~58 kDa (Supporting Note 2 and Supplementary Figure 2). Of note, all the (poly)peptides conjugated in this fashion will display an exposed C-terminus.

Orthogonal Labeling of Three Phage Capsid Proteins. In a first attempt to establish end-to-end phage dimers, we tried to directly link the loopXa-pIII phage and a phage containing a pentaglycine motif at the N-terminus of its pIII (G_5-pIII phage) via $SrtA_{aureus}$. No dimers were observed after 24 h of incubation, and only ~3% of structures were dimeric after 60 h of incubation (Supporting Note 3 and Supplementary Figure 3).

Given the slow kinetics of direct phage−phage fusion using $SrtA_{aureus}$, we hypothesized that the loopXa and pentaglycine motifs on phage could be individually labeled with oligoglycine or LPXTG -based peptides before phage−phage fusions occur. With the ability to label pVIII orthogonally with $SrtA_{pyogenes}$, we created a phage construct (hereafter referred to as triSrt) containing three sortaggable motifs: loopXa on pIII, $(A)_2$ on pVIII, and G_5HA on pIX (all at the N-terminus of the respective proteins). This combination enables selective

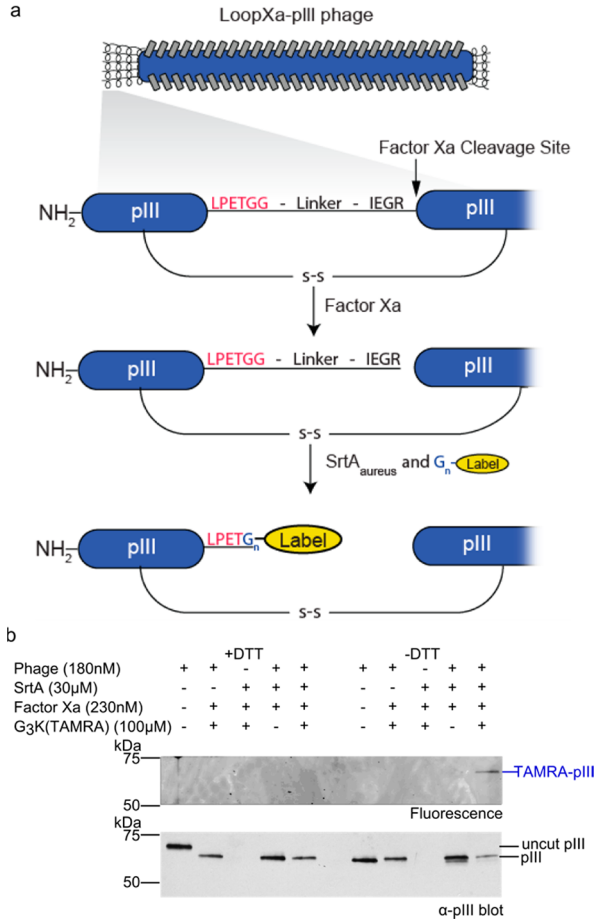

Figure 1. Labeling of loop-pIII. (a) Schematic for C-terminal labeling using the loop structure. (b) LoopXa-pIII phage was incubated with $SrtA_{aureus}$, Factor Xa, and GGGK(TAMRA). The reactions were monitored by SDS-PAGE under reducing and nonreducing conditions followed by fluorescent imaging and immunoblotting with an anti-pIII antibody. The molecular weight markers are shown on the left.

labeling of three proteins on the same phage particle. An HA tag was added to pIX to extend its N-terminus and allow identification of the protein by immunoblot, as no antibodies are commercially available for pIX. We labeled each of these proteins in the triSrt construct with different fluorescent molecules (Figure 2a) in a stepwise manner. First, pVIII was labeled with K(TAMRA)-LPETAA using $SrtA_{pyogenes}$ with subsequent purification of the desired reaction product by PEG8000/NaCl precipitation. The resultant TAMRA-pVIII phage was then incubated with $SrtA_{aureus}$, GGGK-Alexa647, K(FAM)-LPETGG, and Factor Xa for 5 h at room temperature followed by PEG8000/NaCl precipitation. This precipitation allows purification of the labeled virions away from the other reaction components, including the side reaction product K(FAM)-LPETGGGK-Alexa647 resultant from sortase-mediated fusion of the individual fluorescent peptides. Each reaction was analyzed by SDS-PAGE under nonreducing conditions followed by fluorescent imaging and immunoblot using anti-pIII and anti-HA antibodies (Figure 2b). In the final product, we observed a TAMRA fluorescent ~10 kDa protein compatible with the molecular weight of pVIII, an Alexa647 fluorescent and anti-pIII reactive 60 kDa protein (Figure 2b, lanes 4 and 6), plus a FAM-fluorescent and anti-HA (pIX) reactive ~10 kDa protein (Figure 2b, lanes 5 and 6).

dx.doi.org/10.1021/sb400019s | ACS Synth. Biol. 2013, 2, 490−496

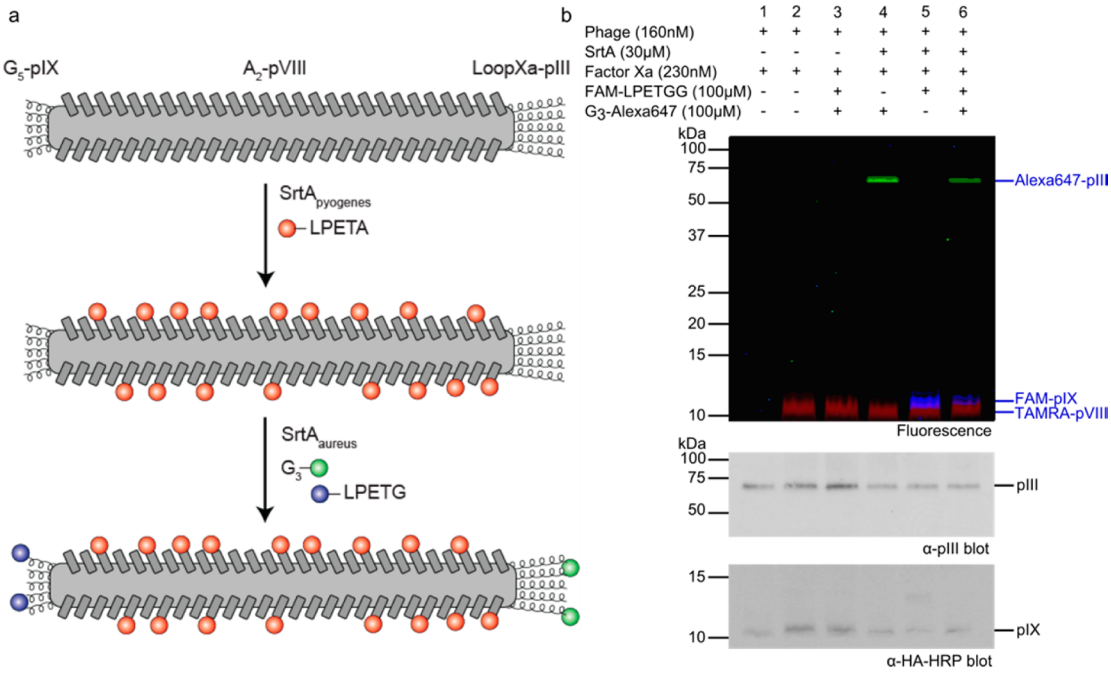

Figure 2. Orthogonal labeling of phage with three fluorophores. (a) Schematic representation of the strategy used for triple labeling of a single phage particle. TriSrt phage (lane 1) was incubated with $SrtA_{pyogenes}$ and K(TAMRA)-LPETAA and purified by PEG8000/NaCl precipitation (lane 2). The TAMRA-pVIII labeled triSrt phage was incubated with Factor Xa, $SrtA_{aureus}$, FAM-LPETGG, and/or G_3-Alexa647 and purified. (b) These reactions were monitored by SDS-PAGE under nonreducing conditions, followed by fluorescent imaging and immunoblotting with an anti-pIII or anti-HA antibody. The molecular weight markers are indicated on the left.

Labeling of pIII and pIX with DNA. Because we can now functionalize the ends of the same phage particle orthogonally with different molecules, we sought to form phage trimers by DNA hybridization (Figure 3a). Thiolated and Cy5-labeled DNA oligonucleotides were conjugated to either a (maleimide)-LPETGG or GGGK(maleimide) peptides (Supplementary Table S1). The resultant DNA-peptide adducts were purified by size exclusion chromatography and analyzed by MALDI-TOF mass spectrometry. The product displayed a size consistent with (maleimide)-LPETGG (~700 Da) and GGGK-(maleimide) (~400 Da) peptides fused to the DNA oligonucleotides (Supplementary Figure 4a). These were also analyzed by TBE-urea PAGE followed by fluorescent imaging (Supplementary Figure 4b). Upon reaction with maleimide-peptides, we observed a shift in mobility of the DNA and did not detect any unreacted DNA, suggesting that all DNA was conjugated to the peptide.

Using $SrtA_{aureus}$ and the triSrt phage, we attached DNA-peptides to pIII and to pIX, forming three different phage constructs: DNA A-pIX phage, DNA B-pIII-DNA D-pIX phage, and DNA E-pIII phage (Figure 3a). The reaction products were purified by PEG8000/NaCl precipitation. Free DNA-peptide coprecipitated with the phage, so an additional dialysis step was performed to remove it. The purified DNA-labeled phage was analyzed by SDS-PAGE under nonreducing conditions, followed by fluorescent imaging (Figure 3b). Labeling of pIX with DNA A and DNA D (Figure 3b, left panel) resulted in detection of Cy5-fluorescent 19 kDa and 22 kDa proteins, respectively. This is consistent with the predicted size of the DNA-pIX species. When pIII was labeled with DNA B and DNA E (Figure 3b, right panel), we detected Cy5-fluorescent 75 kDa and 80 kDa proteins, respectively. These sizes are consistent with those expected for the DNA-pIII species.

Formation of Ordered Phage Trimers. We mixed equimolar amounts of the above DNA-labeled virions, followed by addition of the hybridizing oligonucleotides DNA C and DNA F in 10-fold excess over phage (Supplementary Table S1 and Figure 3a). The mixture was heated at 95 °C and cooled to 20 °C, thus allowing DNA to anneal and connect the phage particles. Atomic force microscopy (AFM) showed that this heating and cooling did not disrupt the integrity of the phage structure. Analysis of the annealed phage structure by AFM showed the existence of multiphage structures of 2−3 μm in length (Figure 3c and Supplementary Figure 5). No structures corresponding to phage particles intersecting with more than one phage at its end were detected, suggesting that the connections were indeed 1:1. We analyzed the phage population, compiling a histogram of the lengths of observed structures (Figure 3d and Supplementary Figure 5). For each treatment, at least 50 structures were measured. The length of a single phage is ~880 nm. We thus assume that a structure <1 μm represents a single phage, 1−2 μm is two connected phage, 2−3 μm is three connected phage, and >3 μm is more than three connected phage. We observed that 52% of phage structures were 2−3 μm. Structures longer than 3 μm were observed rarely (5.8%), the longest observed structure being 4.70 μm. In contrast, when DNA C and DNA F were omitted from the reaction, 95% of the observed phage structures were less than 1 μm and no 2−3 μm structures could be found. Dynamic light scattering (DLS) showed an increase in the distribution of the particle sizes. When DNA C and DNA F were absent, we observed a peak for objects with a radius of ~100 nm, corresponding to phage monomers. The size of the particles in the main peak increased significantly (~1300 nm) when DNA C and DNA F were added. Particles comprising this peak were compatible with trimer structures based on the structures observed by AFM (Figure 3d). Because phage is

dx.doi.org/10.1021/sb400019s | ACS Synth. Biol. 2013, 2, 490−496

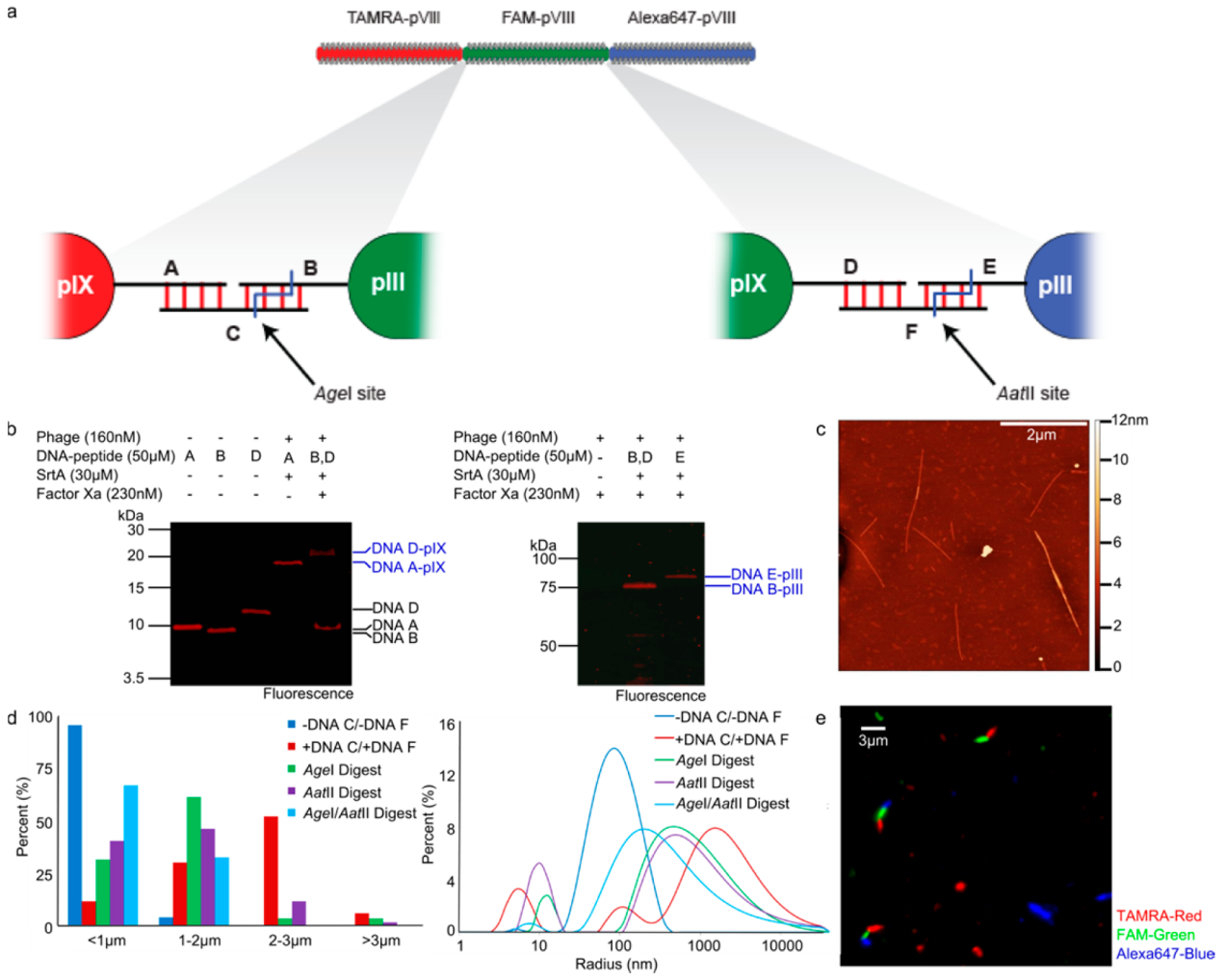

Figure 3. Building phage by DNA hybridization. (a) Scheme of the multiphage final structure upon DNA hybridization. TriSrt Phage was incubated with DNA-peptides and $SrtA_{aureus}$ and purified by PEG8000/NaCl precipitation. (b) The reactions were monitored by SDS-PAGE under nonreducing conditions, followed by fluorescent imaging. The samples with DNA-peptide alone had a concentration of 650 nM instead of 50 μM. The molecular weight markers are shown on the left. (c) Phage were linked (see Methods for details) and imaged by atomic force microscopy. (d) The lengths of the phage structures were measured, collected in a histogram, and analyzed by dynamic light scattering. (e) Fluorescently labeled phage were connected and imaged by fluorescent microscopy.

filamentous and not spherical, the numerical value of the hydrodynamic radii is reported to demonstrate only relative changes in size.

To confirm that the observed multiphage structures were indeed formed by DNA hybridization, we incubated them with restriction enzymes: *Aat*II cleaves the annealed DNA structure between DNA A−C, *Age*I cleaves the connections between DNA D−F (Figure 3a). The samples were analyzed using AFM and DLS (Figure 3d and Supplementary Figure 6). Upon digestion with the individual enzymes, we observed a decrease in the structure length of the 2−3 μm phage particles (12% for *Aat*II, 3.3% for *Age*I), with structures of 1−2 μm in length being the most prevalent (46% for *Aat*II, 62% for *Age*I). This shift was consistent with the size distribution observed by DLS, where the peak for both *Aat*II and *Age*I digest shifted to ∼500 nm, corresponding to dimer phage structures. When the multiphage preparation was incubated with both enzymes, we no longer observed phage structures of 2−3 μm in length and the majority of the population was under 1 μm (67%) (Figure 3d and Supplementary Figure 6). These results were supported by DLS, where the peak of particle sizes decreased to ∼200 nm. We speculate that not all phage particles return to the monomeric form for reasons of steric hindrance: the phage structures themselves shielded the hybridized DNA from the restriction enzymes.

To ensure that the multiphage structures were connected in the desired order, we fluorescently labeled the pVIII of the triSrt phage using $SrtA_{pyogenes}$ with different fluorophores,[7] followed by DNA labeling. This yielded the following phage particles: TAMRA-pVIII-DNA A-pIX, DNA B-pIII-FAM-pVIII-DNA D-pIX, and DNA E-pIII-Alexa647-pVIII. We mixed these phage in equimolar amounts with a 10-fold excess DNA C and F and imaged them by fluorescence microscopy (Figure 3e and Supplementary Figure 7). We observed multicolor filamentous structures connected in the expected order: TAMRA, FAM, and Alexa647 (Figure 3a,e and Supplementary Figure 7). In the absence of DNA, such connected multicolor filamentous structures were not observed and only single-colored filaments were present (Supplementary Figure 7).

dx.doi.org/10.1021/sb400019s | *ACS Synth. Biol.* 2013, 2, 490−496

Conclusions. Here we expand sortase-mediated labeling of M13 bacteriophage by engineering a loop onto pIII to enable C-terminal labeling. The insertion of a cleavable loop allows C-terminal exposure of the sortase motif LPXTG and thus enables attachment of a substituted peptide or protein at that site via exposed Gly residues. Using this new structure, we attach a fluorophore and an oligomeric complex protein, neither of which could ever be displayed on the phage capsid genetically. Engineering of this loop onto pIII enables labeling orthogonal to the previously established N-terminal labeling method.[7,18] Thus, we created a new phage construct with the loop structure on pIII, a pentaglycine motif on pIX, and a double alanine motif on pVIII. Although this configuration should theoretically allow direct phage to phage conjugation, we found this to be an inefficient reaction, possibly for steric reasons, and therefore resorted to the use of complementary DNA crossbridges to achieve our goal. We demonstrated as a proof of concept that the minor capsid proteins of phage can be labeled with DNA and used to form specific connections between different phage particles. This reaction was more efficient, with over 50% of observed phage structures displaying the length of trimers. The precision of this strategy surpasses earlier accomplishments in which phage were linked using leucine zippers: heterodisperse multiphage structures were obtained with mean lengths of 3−4.5 μm (6−8 phage) and variability of length from monomers to longer than 20 phage.[9]

Not only does the DNA modified phage as a scaffold building block allow better control over the structures that can be produced, but this strategy should be readily extendable to create much longer multimers by the proper choice of different DNA sequences. Our work sets the stage for building more complex multiphage structures, such as multiway junctions,[19] or combinations with DNA origami structures[10] with the potential to control positions in three dimensions.[20] Attached DNA may also be used as a functional material sensitive to the environment such as pH[21] or bind substrates through the use of DNA aptamers,[22,23] which extend the properties of the proteins or peptides displayed on the phage capsid, which has potential in biosensing applications.[24]

The specific connection of phage particles, which we demonstrate, provides control of interactions between multiple materials at the nano scale. Although the phage particles connected in this work were identical genetically, we attached different fluorophores to their pVIII body protein to establish that the requisite linkages were being formed in a predetermined order. In principle, the ability to pattern phage with different pVIII proteins enables self-assembly of junctions between materials and formation of multimaterial axial nanowires or even circuits. This ability potentially allows for phage-based devices where configuration and the proximity of materials are critical, including transistor- and diode-based electronic devices.[25,26]

METHODS

Phage Engineering. The oligonucleotides used in engineering phage are shown in Supplementary Table S2. LoopXa-pIII phage was constructed from an M13KE vector (New England Biolabs). The vector was digested with *Acc*65I and *Eag*I. The annealed oligonucleotides pIIILoop-C and pIIILoop-NC were annealed and ligated into the digested vector. The Factor Xa resognition site was introduced by mutagenesis using the Quik II Site-Directed Mutagenesis kit (Stratagene) with oligonucleotides pIIILoopXaTop and pIIILoopXaBottom. The p9G5HA vector phage construct[7] served as template for creating the triSrt phage. The loop containing the Factor Xa recognition site was installed on pIII as described above. Two alanine codons were introduced at the 5′ end of pVIII using *Pst*I and *Bam*HI restriction enzymes and the annealed pVIII-AA-C and pVIII-AA-NC oligonucleotides. The phage constructs were transformed, plated, and amplified as described.[7]

Sortase-Mediated Reactions. Sortase reactions were performed as indicated in the figures. A typical sortase reaction for labeling loopXa-pIII phage consisted of 160 nM phage, 30 μM $SrtA_{aureus}$, 230 nM Factor Xa, 100 μM GGGK(TAMRA) or G_3 fused to the N-terminus of the B subunit of cholera toxin (G_3-CtxB), and 10 mM $CaCl_2$ in TBS (25 mM Tris, pH 7.0−7.4, and 150 mM NaCl) incubated for 5 h at room temperature. The concentration reported for G_3-CtxB is the monomer concentration. The sortase labeling reactions with GGGK-(TAMRA) were monitored by SDS-PAGE under reducing and nonreducing conditions followed by fluorescent imaging and immunoblot with an anti-pIII antibody (New England Biolabs). The CtxB labeling reactions were analyzed by SDS-PAGE in nonreducing conditions followed by immunoblot using an anti-pIII and anti-CtxB antibody (GenWay Biotech).

Typical conditions for labeling the pVIII of the triSrt phage were 160 nM phage, 40 μM $SrtA_{pyogenes}$, and 200 μM fluorophore conjugated LPETAA peptide incubated for 3 h at room temperature followed by PEG8000/NaCl precipitation.[7] The end labeling reactions of pIII and pIX consisted of 160 nM phage, 30 μM $SrtA_{aureus}$, 230 nM Factor Xa, and 100 μM fluorescent peptide or 50 μM DNA peptide in 10 mM $CaCl_2$ incubated for 5 h at room temperature followed by PEG8000/NaCl precipitation. For the DNA-phage reactions, additional purification was performed by dialysis against water with a 1 MDa molecular weight cutoff (Spectrum Laboratories), followed by another round of PEG8000/NaCl precipitation to purify and concentrate the samples.

DNA Peptide Conjugation. The DNA oligonucleotides attached to the ends of phage are shown in Supplementary Table S1. The thiol group on the DNA oligonucleotides was activated overnight with 0.1 M DTT in PBS at 37 °C. The DNA was then purified from excess DTT on a NAP5 column (GE Healthcare) and eluted in water. The solution was dried and resuspended in PBS. (Maleimide)-LPETGG or GGGK-(maleimide) peptide in PBS was added in 2:1 molar excess of the activated DNA and reacted for 5 h at 37 °C. In order to deactivate the excess maleimide, DTT was added to the mixture to give a concentration of 0.1 M DTT and incubated at 37 °C for 15 min. The excess DTT and peptide was removed by purifying the reaction on a NAP5 column. The DNA-peptide was dried under vacuum and resuspended in TBS. The concentration of the DNA-peptide was determined by UV−vis spectrometry using the absorbance at 260 nm. DNA-peptides were analyzed by a Micromass microMX MALDI with a pulsed 337 nm nitrogen laser. Spectra were acquired in positive ion, linear mode with a mass range of 2−30 kDa.

Atomic Force Microscopy and Dynamic Light Scattering. The three DNA labeled phage were mixed together at 7×10^{13} pfu/mL in water. Hybridizing oligonucleotides DNA C and F were added in 10-fold molar excess. The reactions were heated to 95 °C for 5 min and cooled down to 20 °C at 0.5 °C per minute. For restriction enzyme digestion the phage were resuspended in NEB Buffer 4 (50 mM potassium acetate, 20 mM Tris-acetate, 10 mM magnesium acetate, 1 mM DTT, pH

7.9) and incubated at 37 °C for 3 h. We verified that the DTT in the NEB buffer did not disrupt the LoopXa-pIII structure by exposing LoopXa-pIII phage with Factor Xa to the buffer. We analyzed the reactions by SDS-PAGE followed by immunoblot with an anti-pIII antibody and estimated by densitometry that 10% of the LoopXa-pIII structures were disrupted, which represents only one pIII molecule for every two phage suggesting this did not significantly affect the connections.

To visualize the samples by AFM, phage preparations were diluted in water to a concentration of 2×10^{11} pfu/mL. Then 90 μL of the phage solution was deposited on a freshly cleaved mica disc. AFM images were captured on a Nanoscope IV (Digital Instruments) in air using tapping mode. The tips had spring constants of 20−100 N/m driven near their resonant frequency of 200−400 kHz (MikroMasch). The AFM images were analyzed and processed using Gwyddion. The histograms were collected by measuring the length of all phage events observed in seven 20 μm × 20 μm areas.

DLS measurements were obtained with a DynaPro NanoStar (Wyatt Technology). Phage mixtures in NEB buffer 4 were diluted to 1×10^{13} pfu/mL in water. Samples from each experiment were measured 20 times, and the results were averaged by cumulant analysis.

Fluorescence Microscopy. The phage samples were diluted to 6×10^{11} pfu/mL in water, and 300 μL was deposited and dried on a glass coverslip. The samples were imaged using an inverted DeltaVision microscope equipped with an epifluorescent illumination module-488 nm laser (FAM-488 nm) and solid state illumination (TAMRA-543 nm and Alexa647), an oil immersion 100X objective (N.A. = 1.40, 100X, Olympus) and Photometrics CoolSNAP HQ camera. All images were processed using ImageJ program (National Institutes of Health).

Miscellaneous. Expression and purification of $SrtA_{pyogenes}$, $SrtA_{aureus}$, and G_3-CtxB were performed as described.[18] The LoopXa-pIII reactions were analyzed on 10% Laemmli SDS-PAGE gels. The pIX-DNA reactions were analyzed on a 16% Tricine-SDS PAGE gel, and the DNA-peptide conjugation reactions were analyzed on a 10% TBE-urea PAGE gel (Life Technologies). All fluorescent gel images were collected on a Typhoon Trio (GE Healthcare). The GGGK(TAMRA), K(FAM)-LPETGG, GGGK(maleimide), (maleimide)-LPETGG, K(TAMRA)-LPETAA, and K(FAM)-LPETAA peptides were obtained from the Swanson Biotechnology Center. For mass spectrometry, the protein bands of interest were excised, subjected to protease digestion, and analyzed by electrospray ionization tandem mass spectrometry (MS/MS).

■ ASSOCIATED CONTENT

Ⓢ Supporting Information

This material is available free of charge via the Internet at http://pubs.acs.org.

■ AUTHOR INFORMATION

Corresponding Author

*E-mail: ploegh@wi.mit.edu; belcher@mit.edu.

Author Contributions

¶These authors contributed equally to this work.

Notes

The authors declare no competing financial interest.

■ ACKNOWLEDGMENTS

The authors wish to dedicate this paper to the memory of Officer Sean Collier, for his service to and sacrifice for the MIT community. This work was supported by the Institute for Collaborative Biotechnologies through grant W911NF-09-0001 from the U.S. Army Research Office. The content of the information does not necessarily reflect the position or the policy of the Government, and no official endorsement should be inferred. We thank Juan Jose Cragnolini and Jessica Ingram for Alexa647-conjugated peptides. We thank the MIT Biophysical Instrumentation Facility for DLS instrumentation and the Microscopy and Biopolymers & Proteomics Facilities of the Koch Institute Swanson Biotechnology Center for technical support. We thank Eliza Vasile for fluorescence microscopy help, Tom DiCesare for graphics help, and Nimrod Heldman for helpful discussions.

■ ABBREVIATIONS

AFM, atomic force microscopy; CtxB, subunit B of cholera toxin; DLS, dynamic light scattering; FAM, carboxyfluorescein; HA, hemagglutinin; pfu, plaque forming unit; $SrtA_{aureus}$, sortase from *Staphylococcus aureus*; $SrtA_{pyogenes}$, sortase from *Streptococcus pyogenes*; TAMRA, tetramethylrhodamine

■ REFERENCES

(1) Sotiropoulou, S., Sierra-Sastre, Y., Mark, S. S., and Batt, C. A. (2008) Biotemplated Nanostructured Materials. *Chem. Mater. 20* (3), 821−834.

(2) Nam, K. T., Kim, D. W., Yoo, P. J., Chiang, C. Y., Meethong, N., Hammond, P. T., Chiang, Y. M., and Belcher, A. M. (2006) Virus-enabled synthesis and assembly of nanowires for lithium ion battery electrodes. *Science 312* (5775), 885−888.

(3) Lee, Y., Kim, J., Yun, D. S., Nam, Y. S., Shao-Horn, Y., and Belcher, A. (2012) Virus-templated Au and Au/Pt core/shell nanowires and their electrocatalytic activities for fuel cell applications. *Energy Environ. Sci. 5*, 8328−8334.

(4) Dang, X., Yi, H., Ham, M. H., Qi, J., Yun, D. S., Ladewski, R., Strano, M. S., Hammond, P. T., and Belcher, A. M. (2011) Virus-templated self-assembled single-walled carbon nanotubes for highly efficient electron collection in photovoltaic devices. *Nat. Nanotechnol. 6* (6), 377−384.

(5) Lee, Y. J., Yi, H., Kim, W. J., Kang, K., Yun, D. S., Strano, M. S., Ceder, G., and Belcher, A. M. (2009) Fabricating genetically engineered high-power lithium-ion batteries using multiple virus genes. *Science 324* (5930), 1051−1055.

(6) Huang, Y., Chiang, C.-Y., Lee, S. K., Gao, Y., Hu, E. L., Yoreo, J. D., and Belcher, A. M. (2005) Programmable assembly of nanoarchitectures using genetically engineered viruses. *Nano Lett. 5* (7), 1429−1434.

(7) Hess, G. T., Cragnolini, J. J., Popp, M. W., Allen, M. A., Dougan, S. K., Spooner, E., Ploegh, H. L., Belcher, A. M., and Guimaraes, C. P. (2012) M13 bacteriophage display framework that allows sortase-mediated modification of surface-accessible phage proteins. *Bioconjugate Chem. 23* (7), 1478−1487.

(8) Nam, K. T., Peelle, B. R., Lee, S.-W., and Belcher, A. M. (2003) Genetically driven assembly of nanorings based on the M13 virus. *Nano Lett. 4* (1), 23−27.

(9) Sweeney, R. Y., Park, E. Y., Iverson, B. L., and Georgiou, G. (2006) Assembly of multimeric phage nanostructures through leucine zipper interactions. *Biotechnol. Bioeng. 95* (3), 539−545.

(10) Stephanopoulos, N., Liu, M., Tong, G. J., Li, Z., Liu, Y., Yan, H., and Francis, M. B. (2010) Immobilization and one-dimensional arrangement of virus capsids with nanoscale precision using DNA origami. *Nano Lett. 10* (7), 2714−2720.

(11) Cigler, P., Lytton-Jean, A. K. R., Anderson, D. G., Finn, M., and Park, S. Y. (2010) DNA-controlled assembly of a NaTl lattice structure

from gold nanoparticles and protein nanoparticles. *Nat. Mater. 9* (11), 918−922.
(12) Park, S. Y., Lytton-Jean, A. K. R., Lee, B., Weigand, S., Schatz, G. C., and Mirkin, C. A. (2008) DNA-programmable nanoparticle crystallization. *Nature 451* (7178), 553−556.
(13) Nykypanchuk, D., Maye, M. M., van der Lelie, D., and Gang, O. (2008) DNA-guided crystallization of colloidal nanoparticles. *Nature 451* (7178), 549−552.
(14) Xiang, D.-s., Zeng, G.-p., and He, Z.-k. (2011) Magnetic microparticle-based multiplexed DNA detection with biobarcoded quantum dot probes. *Biosens. Bioelectron. 26* (11), 4405−4410.
(15) Goldmann, A. S., Barner, L., Kaupp, M., Vogt, A. P., and Barner-Kowollik, C. (2012) Orthogonal ligation to spherical polymeric microparticles: Modular approaches for surface tailoring. *Prog. Polym. Sci. 37* (7), 975−984.
(16) Race, P. R., Bentley, M. L., Melvin, J. A., Crow, A., Hughes, R. K., Smith, W. D., Sessions, R. B., Kehoe, M. A., McCafferty, D. G., and Banfield, M. J. (2009) Crystal structure of Streptococcus pyogenes sortase A: implications for sortase mechanism. *J. Biol. Chem. 284* (11), 6924−6933.
(17) Guimaraes, C. P., Carette, J. E., Varadarajan, M., Antos, J., Popp, M. W., Spooner, E., Brummelkamp, T. R., and Ploegh, H. L. (2011) Identification of host cell factors required for intoxication through use of modified cholera toxin. *J. Cell Biol. 195* (5), 751−764.
(18) Antos, J. M., Chew, G. L., Guimaraes, C. P., Yoder, N. C., Grotenbreg, G. M., Popp, M. W., and Ploegh, H. L. (2009) Site-specific N- and C-terminal labeling of a single polypeptide using sortases of different specificity. *J. Am. Chem. Soc. 131* (31), 10800−10801.
(19) Cheng, E., Xing, Y., Chen, P., Yang, Y., Sun, Y., Zhou, D., Xu, L., Fan, Q., and Liu, D. (2009) A pH-triggered, fast-responding DNA hydrogel. *Angew. Chem., Int. Ed. 48* (41), 7660−7663.
(20) Ke, Y., Ong, L. L., Shih, W. M., and Yin, P. (2012) Three-dimensional structures self-assembled from DNA bricks. *Science 338* (6111), 1177−1183.
(21) Modi, S., Swetha, M., Goswami, D., Gupta, G. D., Mayor, S., and Krishnan, Y. (2009) A DNA nanomachine that maps spatial and temporal pH changes inside living cells. *Nat. Nanotechnol. 4* (5), 325−330.
(22) Ellington, A. D., and Szostak, J. W. (1992) Selection in vitro of single-stranded DNA molecules that fold into specific ligand-binding structures. *Nature 355* (6363), 850−852.
(23) Song, S., Wang, L., Li, J., Fan, C., and Zhao, J. (2008) Aptamer-based biosensors. *TrAC, Trends Anal. Chem. 27* (2), 108−117.
(24) Lee, J. H., Domaille, D. W., and Cha, J. N. (2012) Amplified protein detection and identification through DNA-conjugated M13 bacteriophage. *ACS Nano 6* (6), 5621−5626.
(25) Kempa, T. J., Tian, B., Kim, D. R., Hu, J., Zheng, X., and Lieber, C. M. (2008) Single and tandem axial pin nanowire photovoltaic devices. *Nano Lett. 8* (10), 3456−3460.
(26) Cui, Y., and Lieber, C. M. (2001) Functional nanoscale electronic devices assembled using silicon nanowire building blocks. *Science 291* (5505), 851−853.